

AD-A220 664

2

OFFICE OF NAVAL RESEARCH

Contract N00014-87-K-0494

R&T Code 400X027YIP

Technical Report No. 9

A Nonlocal Free Energy Density Functional  
Approximation for the Electrical Double Layer

by

L. Mier-y-Teran, S.H. Suh, H.S. White, and H.T. Davis

Prepared for Publication in the  
Journal of Chemical Physics

University of Minnesota  
Department of Chemical Engineering and Materials Science  
Minneapolis, MN 55455

April 10, 1990

Reproduction in whole or in part is permitted for any purpose of the United States  
Government.

This document has been approved for public release and sale; its distribution is unlimited.

DTIC  
ELECTE  
APR 19 1990  
S B D  
Co

90 04 18 013

## REPORT DOCUMENTATION PAGE

|   |       |   |  |  |                    |
|---|-------|---|--|--|--------------------|
| 1a. REPORT SECURITY CLASSIFICATION<br><b>Unclassified</b>   |       |   | 1b. RESTRICTIVE MARKINGS   |  |                    |
| 2a. SECURITY CLASSIFICATION AUTHORITY   |       |   | 3. DISTRIBUTION / AVAILABILITY OF REPORT<br><br><b>Unclassified/Unlimited</b>                        |  |                    |
| 2b. DECLASSIFICATION / DOWNGRADING SCHEDULE   |       |   | 4. PERFORMING ORGANIZATION REPORT NUMBER(S)<br><br><b>ONR Technical Report 9</b>                     |  |                    |
| 5. MONITORING ORGANIZATION REPORT NUMBER(S)   |       |   | 6a. NAME OF PERFORMING ORGANIZATION<br><b>Dept of Chemical Engineering<br/>and Materials Science</b> |  |                    |
| 7a. NAME OF MONITORING ORGANIZATION<br><b>Office of Naval Research</b>  |       |   | 6b. OFFICE SYMBOL<br>(If applicable)<br><b>Code 1113</b>   |  |                    |
| 7b. ADDRESS (City, State, and ZIP Code)<br><b>800 North Quincy Street<br/>Arlington, VA 22217</b>   |       |   | 5c. ADDRESS (City, State, and ZIP Code)<br><b>University of Minnesota<br/>Minneapolis, MN 55455</b>  |  |                    |
| 9. PROCUREMENT INSTRUMENT IDENTIFICATION NUMBER<br><b>Contract No. N00014-87-K-0494</b>   |       |   | 8a. NAME OF FUNDING / SPONSORING ORGANIZATION<br><b>Office of Naval Research</b>                     |  |                    |
| 10. SOURCE OF FUNDING NUMBERS   |       |   | 8b. OFFICE SYMBOL<br>(If applicable)   |  |                    |
| PROGRAM ELEMENT NO.   |       | PROJECT NO.   | TASK NO.   | WORK UNIT ACCESSION NO.  |                    |
| 11. TITLE (Include Security Classification)<br><b>A Nonlocal Free Energy Density Functional Approximation for the Electrical Double Layer</b>   |       |   |  |  |                    |
| 12. PERSONAL AUTHOR(S)<br><b>L. Mier-y-Teran, S.H. Suh, H.S. White, and H.T. Davis</b>  |       |   |  |  |                    |
| 13a. TYPE OF REPORT<br><b>Technical</b>   |       | 13b. TIME COVERED<br><b>FROM 4/10/89 TO 4/10/90</b> |  | 14. DATE OF REPORT (Year, Month, Day)<br><b>April 10, 1990</b> |                    |
| 15. PAGE COUNT<br><b>31</b>   |       |   |  |  |                    |
| 16. SUPPLEMENTARY NOTATION<br><br><b>prepared for publication in the Journal of Chemical Physics</b>  |       |   |  |  |                    |
| 17. COSATI CODES  |       |   | 18. SUBJECT TERMS (Continue on reverse if necessary and identify by block number)                    |  |                    |
| FIELD   | GROUP | SUB-GROUP   |  |  |                    |
|   |       |   |  |  |                    |
|   |       |   |  |  |                    |
| 19. ABSTRACT (Continue on reverse if necessary and identify by block number)<br><br>We construct a free energy density functional approximation for the primitive model of the electrical double layer. The hard sphere term of the free energy functional is based on a nonlocal generic model functional proposed by Percus. This latter model functional, which is a generalization of the exact solution for the non-uniform hard rod model, requires as input the free energy of a homogeneous hard-sphere mixture. We choose the extension of the Carnahan-Starling equation of state to mixtures. The electrostatic part of the non-uniform fluid ion-ion correlations present in the interface, is approximated by that of an homogeneous bulk electrolyte. Using the mean spherical approximation for a neutral electrolyte, we apply the theory to symmetrical 1:1 and 2:2 salts in the restricted primitive model. We present comparisons of density profiles and diffuse layer potentials with Gouy-Chapman theory and Monte Carlo data. When available, we also compare our results with data from other recent theories of the double layer. For highly charged surfaces, the profiles show the layering of counterions and charge inversion effects, in agreement with Monte Carlo data. (KCP) ← |       |   |  |  |                    |
| 20. DISTRIBUTION / AVAILABILITY OF ABSTRACT<br><input checked="" type="checkbox"/> UNCLASSIFIED/UNLIMITED <input type="checkbox"/> SAME AS RPT <input type="checkbox"/> DTIC USERS  |       |   | 21. ABSTRACT SECURITY CLASSIFICATION<br><b>Unclassified</b>  |  |                    |
| 22a. NAME OF RESPONSIBLE INDIVIDUAL<br><b>Henry S. White</b>  |       |   | 22b. TELEPHONE (Include Area Code)<br><b>(612) 625-6995</b>  |  | 22c. OFFICE SYMBOL |

# A NONLOCAL FREE ENERGY DENSITY FUNCTIONAL APPROXIMATION FOR THE ELECTRICAL DOUBLE LAYER.

L. Mier-y-Teran, \* S. H. Suh, H. S. White, and H. T. Davis

Department of Chemical Engineering and Materials Science,  
University of Minnesota, Minneapolis, MN 55455

Submitted to Journal of Chemical Physics (November, 1989).

## ABSTRACT

We construct a free energy density functional approximation for the primitive model of the electrical double layer. The hard sphere term of the free energy functional is based on a nonlocal generic model functional proposed by Percus. This latter model functional, which is a generalization of the exact solution for the non-uniform hard rod model, requires as input the free energy of a homogeneous hard-sphere mixture. We choose the extension of the Carnahan-Starling equation of state to mixtures. The electrostatic part of the non-uniform fluid ion-ion correlations present in the interface, is approximated by that of an homogeneous bulk electrolyte. Using the mean spherical approximation for a neutral electrolyte, we apply the theory to symmetrical 1:1 and 2:2 salts in the restricted primitive model. We present comparisons of density profiles and diffuse layer potentials with Gouy-Chapman theory and Monte Carlo data. When available, we also compare our results with data from other recent theories of the double layer. For highly charged surfaces, the profiles show the layering of counterions and charge inversion effects, in agreement with Monte Carlo data.

|                    |  |
|--------------------|--|
| Accession For      |  |
| NTIS GRA&I         | <input checked="checked" type="checkbox"/> |
| DTIC TAB           | <input type="checkbox"/>                   |
| Unannounced        | <input type="checkbox"/>                   |
| Justification      |  |
| By _____           |  |
| Distribution/      |  |
| Availability Codes |  |
| Dist               | Avail and/or<br>Special                    |
| A-1                |  |

\* On sabbatical leave from Departamento de Fisica, Universidad Autonoma Metropolitana- Iztapalapa, Apartado Postal 55-534, 09340 Mexico, D.F., Mexico

## I. INTRODUCTION

Understanding the behavior of charged particles near charged surfaces is an important problem in physical chemistry. Separation of charge in response to the field of the charged surface is referred to as the electrical double layer. Double layers are present in electrochemistry in the form of the electrode/electrolyte interface, and they often play a major role in the stability of soap films, colloidal dispersions, and biological membranes. As a result of the occurrence of double layers in numerous situations, there has been a considerable effort to describe them theoretically. The early theory that met with significant success was that of Gouy [1] and Chapman [2] and was based on the Poisson-Boltzmann equation. More recently, theory has been built on more rigorous methods of the statistical mechanics of the liquid state [3]. Because the physical systems in which double layers occur are generally quite complicated (for a recent review see Ref. [4]) theoretical efforts have been directed towards determination of the properties of greatly simplified models. The Gouy-Chapman theory [1-2] was developed for a model of point charges next to a uniformly charged planar surface, for example. A later modification of this theory by Stern [5], known as the modified Gouy-Chapman theory (MGC), is based on the same model. This description is quite accurate provided the real ionic radius is not too large compared to ionic spacing and the charge on the surface and on the particles are relatively small (low density-weakly coupled systems). At higher densities or for highly coupled systems, the core interaction becomes important. Thus, to take into account of the finite size of the charged particles, many authors focused their attention on a model electrical double layer composed of charged hard spheres at a hard, planar, polarizable, uniformly charged surface. The ions are assumed to be immersed in a continuum with a dielectric constant which may be different from that of the charged wall. This model is known as the primitive model (PM) of the double layer.

There is a considerable body of recent work on the PM double layer. For testing theory, the Monte Carlo (MC) simulations by Valleau and co-workers [6], are especially significant. There is the work on the modified Poisson-Boltzmann (MPB) approximation [7], which is based on the Kirkwood [3] hierarchy. In that approach the effects of the wall on the ion-ion correlations are handled in a natural way. On the other hand, the work based on the singlet Ornstein-Zernike (OZ) equation [8] with the mean spherical approximation (MSA) or the hypernetted chain approximation (HNC) stresses on a more careful treatment of the effects due to the finite size of the ions while the direct ion-ion correlation functions near the surface are approximated by the functions calculated in the bulk solution [9]. There is also work based on the Born-Green-Yvon (BGY) equation [10-11]. By using phenomenological expressions for the inhomogeneous pair correlation functions as closures for the BGY equation, this latter method emphasizes the importance of properly handling the ion-ion correlation functions near the wall. The BGY equation exactly satisfies the contact theorem [3]. This is especially important in the high density-high coupling regime. The recent work by Fortsmann and collaborators [12,13], in which the ion-ion direct correlation functions are computed using the MSA at a local non-neutral

concentration (HNC/LMSA), is also aimed at building into the theory good pair correlation functions. Similar in spirit to the work of Fortsmann and collaborators is that of Kjellander and Marcelja [14], in which the double layer interaction between two uniformly charged surfaces immersed in an electrolyte solution is calculated. Perhaps the most accurate recent work is that of Plischke and Henderson [15]. In that work, the inhomogeneous OZ equation with the HNC and MSA closures were solved together with the Lovett-Mou-Buff-Wertheim equation [16] for the density profiles of the ions (OZ/LMBW).

Double layers are good examples of strongly inhomogeneous systems. In an electrolyte, especially at elevated surface charges, the density variations near the electrode are extremely large. The situation of an ion near the wall is totally different from that of a similar ion in the neutral bulk. Ideally, a double layer theory should take into account the correlations arising from both the hard-core repulsion and the electrostatic interactions. Because these correlations are strongly dependent on the distance from the wall, only a few theories are able to handle properly the ion packing near the electrode. According to MC results for 1:1 electrolytes [6], at high electrode charges the counterions start the formation of a second layer before the first layer is densely packed. Of the theories mentioned above, only the HNC/LMSA, the BGY, the Kjellander and Marcelja and the OZ/LMBW theories are able to predict the formation of the second layer of counterions.

Parallel to the development of the double layer theories, the last decade has seen a great deal of activity in the study of non-uniform fluids using free energy density functional theories. This method, which originated with van der Waals [17], requires the construction of an expression for the free energy of the inhomogeneous system. Even though the rigorous statistical mechanics formalism of density functional theory was established more than twenty years ago [18,19], the reduction of the exact results to tractable accurate approximations has been the goal of many, more recent investigations [20-26]. Treatments based on local density approximations have proven useful to describe weakly structured systems, like fluid-fluid interfaces [20-22], or fluids in weak external fields, but are not applicable to the strong inhomogeneities characteristic of fluid-solid interfaces. In order to handle the strong inhomogeneities present in fluid-solid interfaces, a nonlocal approach was introduced by Nordholm and coworkers [23] in their generalized van der Waals theory (GVDW). Since then, systematic improvements in the method in which finite size effects are considered have been published [24,26]. Applications of nonlocal theories include the studies of the structure of confined fluids [27-30], capillary condensation [31,32], layering transitions [33], and the planar electrical double layer [34]. Very recently, the nonlocal smoothed-density approach (SDA) due to Tarazona [24], was extended to binary hard sphere mixtures with arbitrary size ratio [35].

In this work, we present a theory for the electrical double layer in which the effects due to the finite size of the particles are considered within the framework of a generic nonlocal functional proposed by Percus [36] and generalized to multicomponent fluids by Vanderlick *et al.* [29]. This generic functional can be used to generate the functionals of several known nonlocal approaches [30]. These include the GVDW, the SDA, and a functional proposed

by Robledo and Varea [37], and by Fischer and Heinbuch [38], as a generalization of Percus' exact solution of the one dimensional hard-rod system [39]. We use the latter, termed here generalized hard-rod model (GHRM), to construct a model functional for the electrical interface. Its advantage over the OZ/LMBW theory used by Plischke and Henderson is that its working equations are much cheaper to evaluate.

The article is as follows. The PM of a planar double layer is described in Sec. II. The general free energy density functional formalism for the electrical double layer is presented in Sec. III. In Sec. IV we report our results for the density profiles and electrostatic potential and compare these with the MC results of Valleau and co-workers [6] and with results of some of the theories mentioned above.

## II. PRIMITIVE MODEL

In the primitive model of the electrical double layer, the electrolyte is assumed to be a fluid of charged hard spheres of charge  $q_\alpha$  and diameter  $d_\alpha$  immersed in a dielectric continuum of dielectric constant  $\epsilon$ . Separating the Coulombic and short-range repulsive contributions to the pair interaction, we have

$$u_{\alpha\beta}(\mathbf{r}, \mathbf{r}') = q_\alpha q_\beta u^c(|\mathbf{r} - \mathbf{r}'|) + u_{\alpha\beta}^r(|\mathbf{r} - \mathbf{r}'|), \quad (2.1)$$

where

$$u^c(r) = 1/\epsilon r, \quad (2.2)$$

and

$$\begin{aligned} u_{\alpha\beta}^r(r) &= \infty, & r < (d_\alpha + d_\beta)/2 \\ &= 0, & r > (d_\alpha + d_\beta)/2. \end{aligned} \quad (2.3)$$

The electrode is considered to be an infinite flat hard wall with a uniform charge density  $\sigma$ . This impenetrable hard wall produces a repulsive potential, for particles of species  $\alpha$ , of the form

$$\begin{aligned} v_\alpha^r(x) &= \infty, & x < d_\alpha/2, \\ &= 0, & x > d_\alpha/2, \end{aligned} \quad (2.4)$$

where  $x$  is the ion's distance to the plate. On the other hand, the uniform surface charge density gives rise to a Coulombic potential of the following form

$$v^c(x) = -2\pi\sigma |x|/\epsilon + C, \quad (2.5)$$

where  $C$  is a constant which depends on the choice of the point of zero potential.

In order to eliminate image charges, the dielectric constant is also taken to be  $\epsilon$  in the region  $x \leq d_\alpha/2$ . The total external potential can now be written as

$$v_\alpha(x) = q_\alpha v^c(x) + v_\alpha^r(x). \quad (2.6)$$

A quantity of an enormous importance in the electrical double layer theory is the mean electrostatic potential. The mean electrostatic potential  $\psi(\mathbf{r})$  at a point  $\mathbf{r}$  is related to the density distribution functions  $n_\alpha(x)$  in the following way

$$\psi(\mathbf{r}) = v^c(x) + \int d^3r' u^c(|\mathbf{r} - \mathbf{r}'|) \sum_\alpha q_\alpha n_\alpha(x'). \quad (2.7)$$

The formal solution to Poisson's equation yields the following expression for the mean electrostatic potential

$$\psi(x) = \frac{4\pi}{\epsilon} \int_x^\infty dx' (x - x') \sum_\alpha q_\alpha n_\alpha(x'). \quad (2.8)$$

The boundary conditions used in arriving at Eq.(2.8) are  $\psi(\infty) = 0$ , and

$$\left. \frac{d\psi(x)}{dx} \right|_{x=0} = \frac{-4\pi\sigma}{\epsilon} \quad (2.9)$$

In the derivation of Eq. (2.8) we required

$$\int_0^\infty dx' \sum_\alpha q_\alpha n_\alpha(x') = -\sigma, \quad (2.10)$$

which is the constraint of overall electroneutrality of the system. From Eq. (2.8) we can observe why the mean electrostatic potential evaluated at the closest approach distance is frequently used as a measure of the charge separation in the double layer.

### III. DENSITY FUNCTIONAL FREE ENERGY THEORY

#### General formalism

We start our study of the double layer problem with a discussion of the grand canonical density functional formalism for a mixture of ionic species in an external field. In this work we adopt the general approach due to Morita and Hiroike [40], De Dominicis [41], Stillinger and Buff [42] and to Lebowitz and Percus [43], and used later by many investigators [20-22,44]. The particle-particle direct correlation functions of a non-uniform fluid which appear in the formalism allow us to write an exact expression for the density distribution functions. The same formalism has been used by Fortsmann and collaborators [13] as the starting point of their HNC/LMSA theory of the double layer. This approach, which is due to Mermin [45] and was employed by Hohenberg and Kohn [46] for the inhomogeneous electron gas, is naturally expressed in the language of the grand canonical ensemble.

The properties of an interface and its coexisting bulk fluid are determined by the constancy of the chemical potentials,  $\mu_\alpha$ , and temperature,  $T$ , throughout the system. The

free energy appropriate to the grand canonical ensemble is the grand potential. For a mixture of particles of different kinds ( $\alpha = 1, \dots, c$ ), the grand potential functional is

$$\Omega = -kT \ell n \Xi, \quad (3.1)$$

where  $\Xi$  is the grand partition function and  $k$  is Boltzmann's constant. The equilibrium density distribution is an unconstrained minimum of the grand potential functional,  $\Omega$ , where

$$\Omega(\{n\}) = F(\{n\}) - \sum_{\alpha} \int d^3r \mu_{\alpha} n_{\alpha}(\mathbf{r}). \quad (3.2)$$

Here,  $F(\{n\})$  is the Helmholtz free energy functional of the system and  $\{n\}$  denotes the functional dependence of  $\Omega$  and  $F$  on the particle densities,  $n_{\alpha}(\mathbf{r})$ ,  $\alpha = 1, \dots, c$ .

For a mixture of charged particles of species at absolute temperature  $T$  in the field of an external potential  $v_{\alpha}(\mathbf{r})$ , the grand potential functional can be written as

$$\begin{aligned} \Omega(\{n\}) = & \sum_{\alpha} \int d^3r n_{\alpha}(\mathbf{r}) (v_{\alpha}(\mathbf{r}) - \mu_{\alpha}) \\ & + kT \sum_{\alpha} \int d^3r n_{\alpha}(\mathbf{r}) [\ell n(\Lambda_{\alpha}^3 n_{\alpha}(\mathbf{r})) - 1] - \phi(\{n\}). \end{aligned} \quad (3.3)$$

The second term on the rhs of Eq.(3.3) is the ideal gas contribution to the Helmholtz free energy and  $\Lambda_{\alpha}$  is the thermal de Broglie wavelength of particles  $\alpha$ . The term  $-\phi$  in the same equation corresponds to the interparticle interaction contribution to the free energy.

The grand potential functional  $\Omega(\{n\})$  is minimized, for fixed  $v_{\alpha}(\mathbf{r})$  and  $u_{\alpha\beta}(\mathbf{r}, \mathbf{r}')$ , when  $n_{\alpha}(\mathbf{r})$  takes its equilibrium value. In that case,  $\Omega$  corresponds to the equilibrium grand potential function. The functional  $-\phi$ , on the other hand, can be used as a generating functional for  $n$ -body correlation functions, in particular, from the first functional derivative we obtain:

$$\frac{1}{kT} \frac{\delta \phi(\{n\})}{\delta n_{\alpha}(\mathbf{r})} = c_{\alpha}(\mathbf{r}; \{n\}), \quad (3.4)$$

while the second functional derivative of  $\phi(\{n\})$  defines the Ornstein-Zernike direct correlation function

$$\frac{1}{kT} \frac{\delta^2 \phi(\{n\})}{\delta n_{\alpha}(\mathbf{r}) \delta n_{\beta}(\mathbf{r})} = c_{\alpha\beta}(\mathbf{r}, \mathbf{r}'; \{n\}). \quad (3.5)$$

The equilibrium condition can then be expressed as

$$\frac{\delta \Omega(\{n\})}{\delta n_{\alpha}(\mathbf{r})} = kT \ell n(n_{\alpha}(\mathbf{r})/\zeta_{\alpha}) + v_{\alpha}(\mathbf{r}) - kT c_{\alpha}(\mathbf{r}; \{n\}) = 0, \quad (3.6)$$

where  $\zeta_{\alpha} = \Lambda_{\alpha}^{-3} \exp(\beta \mu_{\alpha})$  is the fugacity of component  $\alpha$  in the mixture and  $\beta = 1/kT$ .



By functional integration between an initial state  $\mathbf{n}^i$ , and a final state  $\mathbf{n}$ , it is possible to obtain

$$\begin{aligned}\phi(\{\mathbf{n}\}) &= \phi(\{\mathbf{n}^i\}) + kT \sum_{\alpha} \int d^3r [n_{\alpha}(\mathbf{r}) - n_{\alpha}^i(\mathbf{r})] c_{\alpha}(\mathbf{r}; \{\mathbf{n}^i\}) \\ &+ kT \sum_{\alpha\beta} \int \int d^3r d^3r' [n_{\alpha}(\mathbf{r}) - n_{\alpha}^i(\mathbf{r})] \\ &\times [n_{\beta}(\mathbf{r}') - n_{\beta}^i(\mathbf{r}')] \int_0^1 d\lambda \int_0^{\lambda} d\lambda' c_{\alpha\beta}(\mathbf{r}, \mathbf{r}'; \lambda').\end{aligned}\quad (3.7)$$

In order to obtain this result, the linear density path,

$$n_{\alpha}(\mathbf{r}; \lambda) = n_{\alpha}^i(\mathbf{r}) + \lambda[n_{\alpha}(\mathbf{r}) - n_{\alpha}^i(\mathbf{r})],$$

was used for the integration. The parameter  $\lambda$  can take values in the interval  $0 \leq \lambda \leq 1$ . Equations (3.3), (3.6) and (3.7) can now be employed to write the following expression for the grand potential functional:

$$\begin{aligned}\Omega(\{\mathbf{n}\}) &= \Omega(\{\mathbf{n}^i\}) + \sum_{\alpha} \int d^3r n_{\alpha}(\mathbf{r}) [v_{\alpha}(\mathbf{r}) - v_{\alpha}^i(\mathbf{r})] \\ &+ kT \sum_{\alpha} \int d^3r n_{\alpha}(\mathbf{r}) \ln(n_{\alpha}(\mathbf{r})/n_{\alpha}^i(\mathbf{r})) \\ &- kT \sum_{\alpha} \int d^3r [n_{\alpha}(\mathbf{r}) - n_{\alpha}^i(\mathbf{r})] \\ &- kT \sum_{\alpha\beta} \int \int d^3r d^3r' [n_{\alpha}(\mathbf{r}) - n_{\alpha}^i(\mathbf{r})] [n_{\beta}(\mathbf{r}') - n_{\beta}^i(\mathbf{r}')] \\ &\times \int_0^1 d\lambda \int_0^{\lambda} d\lambda' c_{\alpha\beta}(\mathbf{r}, \mathbf{r}'; \lambda').\end{aligned}\quad (3.8)$$

When dealing with long-ranged Coulombic potentials it is convenient to define a short-range part of the direct correlation function  $c_{\alpha\beta}^{SR}(\mathbf{r}, \mathbf{r}')$  by

$$c_{\alpha\beta}(\mathbf{r}, \mathbf{r}') = -\beta q_{\alpha} q_{\beta} u^c(|\mathbf{r} - \mathbf{r}'|) + c_{\alpha\beta}^{SR}(\mathbf{r}, \mathbf{r}').\quad (3.9)$$

The short-range correlation function,  $c_{\alpha\beta}^{SR}(\mathbf{r}, \mathbf{r}')$ , can be further separated by subtracting from it the hard-sphere contribution,  $c_{\alpha\beta}^{HS}(\mathbf{r}, \mathbf{r}')$ . This is,

$$\Delta c_{\alpha\beta}(\mathbf{r}, \mathbf{r}') = c_{\alpha\beta}(\mathbf{r}, \mathbf{r}') - c_{\alpha\beta}^{HS}(\mathbf{r}, \mathbf{r}').\quad (3.10)$$

These definitions allow us to rewrite the grand free energy functional as

$$\begin{aligned}
\Omega(\{\mathbf{n}\}) = & \Omega(\{\mathbf{n}^i\}) + \sum_{\alpha} \int d^3r n_{\alpha}(\mathbf{r}) [v_{\alpha}(\mathbf{r}) - v_{\alpha}^i(\mathbf{r})] \\
& + kT \sum_{\alpha} \int d^3r n_{\alpha}(\mathbf{r}) \ln(n_{\alpha}(\mathbf{r})/n_{\alpha}^i(\mathbf{r})) \\
& - kT \sum_{\alpha} \int d^3r [n_{\alpha}(\mathbf{r}) - n_{\alpha}^i(\mathbf{r})] \\
& + \frac{1}{2} \sum_{\alpha\beta} \int \int d^3r d^3r' [n_{\alpha}(\mathbf{r}) - n_{\alpha}^i(\mathbf{r})] [n_{\beta}(\mathbf{r}') - n_{\beta}^i(\mathbf{r}')] q_{\alpha} q_{\beta} u^c(|\mathbf{r} - \mathbf{r}'|) \\
& - kT \sum_{\alpha\beta} \int \int d^3r d^3r' [n_{\alpha}(\mathbf{r}) - n_{\alpha}^i(\mathbf{r})] [n_{\beta}(\mathbf{r}') - n_{\beta}^i(\mathbf{r}')] \\
& \times \int_0^1 d\lambda \int_0^{\lambda} d\lambda' \Delta c_{\alpha\beta}(\mathbf{r}, \mathbf{r}'; \lambda') + \Delta F^{HS}(\{\mathbf{n}\}).
\end{aligned} \tag{3.11}$$

The last term on the right hand side of Eq.(3.11) represents the excess free energy change, between the initial state  $\mathbf{n}^i$ , and the final state  $\mathbf{n}$ , produced by the hard sphere interaction exclusively (in the presence of the other interactions).

Using the equilibrium condition, Eq.(3.6), we can obtain the following formal expression for the equilibrium density profiles  $n_{\alpha}(\mathbf{r})$ :

$$\begin{aligned}
kT \ln(n_{\alpha}(\mathbf{r})/n_{\alpha}^i(\mathbf{r})) = & -(v_{\alpha}^r(\mathbf{r}) - v_{\alpha}^i(\mathbf{r})) - q_{\alpha}(\psi(\mathbf{r}) - \psi^i(\mathbf{r})) \\
& + kT \sum_{\beta} \int d^3r' [n_{\beta}(\mathbf{r}') - n_{\beta}^i(\mathbf{r}')] \int_0^1 d\lambda \Delta c_{\alpha\beta}(\mathbf{r}, \mathbf{r}'; \lambda) \\
& - \frac{\delta \Delta F^{HS}(\{\mathbf{n}\})}{\delta n_{\alpha}(\mathbf{r})}.
\end{aligned} \tag{3.12}$$

In the derivation of Eq(3.12) use has been made of the definition of the mean electrostatic potential, Eq. (2.7).

### Generalized hard-rod model

The formalism presented above must be completed by specification of a model functional for the excess free energy of a hard-sphere mixture. Generalizing the exact result for an inhomogeneous system of hard-rods, Percus [36] and Vanderlick *et al.* [29] have defined a generic free energy functional for the inhomogeneous hard sphere fluid. In three dimensions, the free energy function of a hard sphere mixture is [29]

$$F^{excess} = \sum_{\alpha} \int d^3r \bar{n}_{\alpha}^{\nu}(\mathbf{r}) F_o(\{\bar{\mathbf{n}}^r(\mathbf{r})\}), \tag{3.13}$$

where  $F_0(\{n(\mathbf{r})\})$  is the excess free energy per particle of a homogeneous mixture of hard spheres evaluated at the position  $\mathbf{r}$  and  $\bar{n}^\nu(\mathbf{r})$  and  $\bar{n}^\tau(\mathbf{r})$  are coarse grain densities. Each one of these densities is defined by a weighting function of the relative position to the hard sphere center, and, in the most general case, is also a functional of the density distribution,

$$\bar{n}_\alpha^\nu(\mathbf{r}) = \int d^3r' \nu_\alpha(\mathbf{r} - \mathbf{r}'; \{\mathbf{n}\}) n_\alpha(\mathbf{r}'), \quad (3.14)$$

$$\bar{n}_\alpha^\tau(\mathbf{r}) = \int d^3r' \tau_\alpha(\mathbf{r} - \mathbf{r}'; \{\mathbf{n}\}) n_\alpha(\mathbf{r}'). \quad (3.15)$$

Use of definitions (3.14) and (3.15) for a uniform fluid mixture gives the following normalization conditions:

$$\int d^3r \nu_\alpha(\mathbf{r} - \mathbf{r}'; \{\mathbf{n}\}) = \int d^3r \tau_\alpha(\mathbf{r} - \mathbf{r}'; \{\mathbf{n}\}) = 1. \quad (3.16)$$

In order to establish a theory for strongly inhomogeneous fluids based on Eqs.(3.12)-(3.16), a particular form for the weighting functions  $\nu$  and  $\tau$  must be specified. The assignment of weighting functions generates different model density functionals. A discussion of how different appropriate selections of weighting functions generate several important model functionals can be found in Ref.(30). Of particular importance for this work are the forms of  $\nu(\mathbf{r})$  and  $\tau(\mathbf{r})$  proposed by Robledo and Varea [37], and by Fischer and Heinbuch [38] as three dimensional generalizations of the hard-rod model. This model, termed here Generalized Hard Rod Model (GHRM), is characterized by the following weighting functions:

$$\nu_\alpha(\mathbf{r} - \mathbf{r}') = \delta((d_\alpha/2) - |\mathbf{r} - \mathbf{r}'|) / (4\pi(d_\alpha/2)^2), \quad (3.17)$$

$$\tau_\alpha(\mathbf{r} - \mathbf{r}') = H((d_\alpha/2) - |\mathbf{r} - \mathbf{r}'|) / (4\pi(d_\alpha/2)^3/3), \quad (3.18)$$

where  $d_\alpha$  is the diameter of the particles in the fluid,  $\delta(r)$  is the Dirac delta function, and  $H(r)$  is the Heaviside step function:

$$\begin{aligned} H(r) &= 1, & r &\geq 0, \\ &= 0, & r &\leq 0. \end{aligned} \quad (3.19)$$

In this model, the coarse grain density  $\bar{n}_\alpha^\nu(\mathbf{r})$  is the average density of species over the surface of a sphere of radius  $d_\alpha/2$ . The coarse-grain density  $\bar{n}_\alpha^\tau(\mathbf{r})$  is the average density of species inside a sphere of radius  $d_\alpha/2$ .

The functional in Eq. (3.13) allows us to determine an expression for the free energy change  $\Delta F^{HS}(\{\mathbf{n}\})$  appearing in Eq.(3.11). It is

$$\Delta F^{HS}(\{\mathbf{n}\}) = \sum_\alpha \int d^3r \int_0^1 d\lambda \frac{\partial}{\partial \lambda} (\bar{n}_\alpha^\nu(\mathbf{r}; \lambda) F_0(\{\bar{n}^\tau(\mathbf{r}; \lambda)\})). \quad (3.20)$$

Using this expression we can finally rewrite our equation for the equilibrium density profiles, Eq.(3.12), as

$$\begin{aligned}
kT \ln(n_\alpha(\mathbf{r})/n_\alpha^i(\mathbf{r})) = & -(v_\alpha^r(\mathbf{r}) - v_\alpha^i(\mathbf{r})) - q_\alpha(\psi(\mathbf{r}) - \psi^i(\mathbf{r})) \\
& + kT \sum_\beta \int d^3 r' [n_\beta(\mathbf{r}') - n_\beta^i(\mathbf{r}')] \int_0^1 d\lambda \Delta c_{\alpha\beta}(\mathbf{r}, \mathbf{r}'; \lambda) \\
& - \sum_\beta \int d^3 r' \int_0^1 d\lambda \frac{\partial}{\partial \lambda} \left[ \frac{\delta \bar{n}_\beta^v(\mathbf{r}'; \lambda)}{\delta n_\alpha(\mathbf{r})} F_o(\{\bar{\mathbf{n}}^r(\mathbf{r}'); \lambda\}) \right] \\
& - \sum_\beta \int d^3 r' \int_0^1 d\lambda \frac{\partial}{\partial \lambda} \left[ \bar{n}_\beta^v(\mathbf{r}) \sum_\gamma \frac{\partial F_o(\{\bar{\mathbf{n}}^r(\mathbf{r}'); \lambda\})}{\partial \bar{n}_\gamma^r(\mathbf{r}')} \frac{\delta \bar{n}_\gamma^r(\mathbf{r}'; \lambda)}{\delta n_\alpha(\mathbf{r})} \right].
\end{aligned} \tag{3.21}$$

To study a bulk fluid in equilibrium with a planar electrode we now identify the initial state  $\{\mathbf{n}^i\}$  with the neutral bulk electrolyte. This corresponds to an homogeneous solution in which no external forces are present. Since we are considering an infinite plane with uniform charge density, local densities vary only in the direction  $x$  normal to the wall. Additionally, Eq.(3.21) requires the knowledge of inhomogeneous direct correlation function in excess over the hard sphere,  $\Delta c_{\alpha\beta}(\mathbf{r}, \mathbf{r}')$ , for all the possible positions  $\mathbf{r}$  and  $\mathbf{r}'$  across the interface. Since these correlation functions are not known, we approximate the function  $\Delta c_{\alpha\beta}(\mathbf{r}, \mathbf{r}')$  with the function  $\Delta c_{\alpha\beta}(|\mathbf{r} - \mathbf{r}'|)$  of the homogeneous neutral bulk electrolyte in equilibrium with the interface, this is

$$\Delta c_{\alpha\beta}(\mathbf{r}, \mathbf{r}'; \lambda) \cong \Delta c_{\alpha\beta}(\mathbf{r}, \mathbf{r}'; \lambda = 0) = \Delta c_{\alpha\beta}(|\mathbf{r} - \mathbf{r}'|). \tag{3.22}$$

It is convenient to emphasize here that  $\Delta c_{\alpha\beta}(|\mathbf{r} - \mathbf{r}'|)$  is a pair correlation function for a neutral bulk electrolyte whereas the interface is locally non-neutral. With this approximation, and by using Eqs (3.14) and (3.15) for the GHRM, Eq.(3.21) can be rewritten, for a planar symmetry, as

$$\begin{aligned}
n_\alpha(x)/n_\alpha = & \exp\{-\beta q_\alpha \psi(x) \\
& - \int_0^\infty dx' \nu_{x\alpha}(x - x') \beta F_o(\{\bar{\mathbf{n}}^r(x')\}) + \beta F_o(\mathbf{n}) \\
& - \sum_\beta \int_0^\infty dx' \bar{n}_\beta^v(x') \frac{\partial \beta F_o(\{\bar{\mathbf{n}}^r(x')\})}{\partial \bar{n}_\alpha^r(x')} \tau_{x\beta}(x - x') + \sum_\beta n_\beta \frac{\partial \beta F_o(\mathbf{n})}{\partial n_\alpha} \\
& + \sum_\beta \int d^3 r' [n_\beta(x') - n_\beta] \Delta c_{\alpha\beta}(|\mathbf{r} - \mathbf{r}'|; \{\mathbf{n}\}), \\
& \text{for } x < d_\alpha/2,
\end{aligned} \tag{3.23}$$

and

$$n_\alpha(x) = 0, \text{ for } x > d_\alpha/2.$$

For the planar symmetry the coarse grain densities  $\bar{n}_\alpha^\nu(x)$  and  $\bar{n}_\alpha^r(x)$  can be written as

$$\bar{n}_\alpha^\nu(x) = \int \nu_{x\alpha}(x - x') n_\alpha(x') dx', \quad (3.24)$$

and

$$\bar{n}_\alpha^r(x) = \int \tau_{x\alpha}(x - x') n_\alpha(x') dx', \quad (3.25)$$

where the reduced weighting functions  $\nu_{x\alpha}$  and  $\tau_{x\alpha}$ , are defined by

$$\nu_{x\alpha}(x) = \int \int \nu_\alpha(\mathbf{r}) dy dz, \quad (3.26)$$

$$\tau_{x\alpha}(x) = \int \int \tau_\alpha(\mathbf{r}) dy dz. \quad (3.27)$$

After integration over coordinates  $y$  and  $z$ , we obtain, for the GHRM,

$$\nu_{x\alpha}(x) = H((d_\alpha/2) - |x|)/d_\alpha, \quad (3.28)$$

$$\tau_{x\alpha}(x) = 6H((d_\alpha/2) - |x|)((d_\alpha/2)^2 - x^2)/d_\alpha^3. \quad (3.29)$$

We approximate now the excess free energy per particle  $F_o$  of the homogeneous hard-sphere fluid by the Carnahan-Starling equation of state [47]. This equation was generalized to a mixture of hard spheres of different sizes by Mansoori et al. [48]. The expression for the free energy is

$$\begin{aligned} \frac{F_o}{kT} = & \frac{-3}{2}(1 - y_1 + y_2 + y_3) + (3y_2 + 2y_3)(1 - \xi)^{-1} \\ & + \frac{3}{2}(1 - y_1 - y_2 - \frac{1}{3}y_3)(1 - \xi)^{-2} + (y_3 - 1)\ln(1 - \xi) \end{aligned} \quad (3.30)$$

where

$$\xi = \sum_\alpha \xi_\alpha, \quad \xi_\alpha = v_\alpha n_\alpha, \quad v_\alpha = \frac{\pi}{6} d_\alpha^3. \quad (3.31)$$

The variables  $y_1$ ,  $y_2$ , and  $y_3$  are defined as follows:

$$y_1 \equiv \frac{1}{2} \sum_{\alpha\beta} \Delta_{\alpha\beta} (d_\alpha + d_\beta) / (d_\alpha d_\beta)^{1/2}, \quad (3.32)$$

$$y_2 \equiv \frac{1}{2} \sum_{\alpha\beta} \Delta_{\alpha\beta} (d_\alpha d_\beta)^{\frac{1}{2}} \sum_\gamma \xi_\gamma / (\xi d_\gamma), \quad (3.33)$$

$$y_3 \equiv \left[ \sum_\alpha (\xi_\alpha / \xi)^{\frac{1}{2}} (n_\alpha / n)^{\frac{1}{2}} \right]^3, \quad (3.34)$$

and

$$\Delta_{\alpha\beta} \equiv (v_{\alpha}v_{\beta})^{\frac{1}{2}} n_{\alpha}n_{\beta}(d_{\alpha} - d_{\beta})^2/(\xi n d_{\alpha}d_{\beta}). \quad (3.35)$$

In the last two equations,  $n$  is the total number density given by  $\sum_{\alpha} n_{\alpha}$ .

In their study of fluids confined between planar walls, Vanderlick et al. [30] compared three different approximate density functional free energy theories of inhomogeneous fluids for hard spheres and Lennard-Jones potentials. Their study included the GHRM and the SDA due to Tarazona [24]. The results of that study show that whereas the GHRM is quantitatively inferior to the SDA, it is qualitatively correct. Since the GHRM captures the qualitative behavior of confined hard-sphere and Lennard-Jones fluids and retains enough mathematical simplicity we are encouraged to apply it to more complicated systems.

### MSA Approximation for $\Delta c_{\alpha\beta}(|\mathbf{r} - \mathbf{r}'|)$

It follows from Eq.(3.23) that our description of the electrical planar interface is still not complete without a prescription for bulk phase direct correlation functions  $\Delta c_{\alpha\beta}(|\mathbf{r} - \mathbf{r}'|)$ . Several choices can be immediately invoked from bulk electrolyte theory. A simple choice is to use the direct correlation functions of the MSA. The MSA is a relatively accurate approximation which generates analytic expressions for the direct correlation function of several important model potentials [49]. Waismann and Lebowitz [50] showed that the integral equation resulting from the Ornstein-Zernike equation, has an analytical solution when the MSA closure for the restricted primitive model(RPM) is employed. The RPM is a still simpler model in which all ions have the same size;  $d_{\alpha} = d$ . For the RPM, the MSA provide the following expression for the function  $\Delta c_{\alpha\beta}(|\mathbf{r} - \mathbf{r}'|)$ :

$$\begin{aligned} \Delta c_{\alpha\beta}(s) &= \frac{-\beta q_{\alpha}q_{\beta}}{\epsilon} [(2B/d) - (B/d)^2 s - 1/s], s < d \\ &= 0 \quad s > d, \end{aligned} \quad (3.36)$$

where  $s = |\mathbf{r} - \mathbf{r}'|$  and

$$B = [\varphi + 1 - (1 + 2\varphi)^{\frac{1}{2}}]/\varphi, \quad (3.37)$$

and  $\phi = \kappa_D d$ . The quantity  $\kappa_D$  is the inverse Debye screening length given by

$$\kappa_D^2 = (4\pi\beta/\epsilon) \sum_{\alpha}^c n_{\alpha}q_{\alpha}^2. \quad (3.38)$$

The solution given by Eq.(3.36) holds for an arbitrary number,  $c$ , of ionic species provided global charge neutrality is maintained,

$$\sum_{\alpha}^c n_{\alpha}q_{\alpha} = 0. \quad (3.39)$$

The MSA direct correlation function is an important piece in the formulation of the HNC/MSA theory of the double layer [9]. In that theory, the approximation

$$c_{\alpha\beta}(\mathbf{r}, \mathbf{r}'; \lambda) \cong c_{\alpha\beta}(\mathbf{r}, \mathbf{r}'; \lambda = 0) = c_{\alpha\beta}(|\mathbf{r} - \mathbf{r}'|) \quad (3.40)$$

is made; thus, the effect of the external potential and the inhomogeneities of the interface on  $c(\mathbf{r}, \mathbf{r}')$  are entirely neglected. We believe that this approximation is more severe than the similar approximation of Eq.(3.22) used in this work.

#### IV. RESULTS

In this section we present our results for the density profiles, mean electrostatic potential profile, and diffuse layer potential drop for solutions containing symmetrical 1:1 and 2:2 electrolytes. The results are compared with existing MC data and, when possible, with results obtained from several other approximations. The calculations were performed by means of the method of subdomains, finite element basis functions, collocation weighted residuals, [51] and Newton iteration with initialization chosen by parametric continuation [52]. We choose quadratic Lagrange interpolating polynomials as basis functions. This numerical technique was applied before to the solution of PY, HNC [52] and MSA [53] integral equations for bulk simple fluids and was extended by Mier y Teran et al. [9] for solving the HNC/MSA integral equation for the double layer problem. A detailed comparative discussion about the application of this method to the solution of HNC/MSA equation for the double layer RPM and its efficiency and accuracy can be found in Ref.(54).

With the algorithm mentioned above, we reduced the set of Eqs.(3.23) to a system of algebraic equations for the values of reduced density profiles at the nodes:  $g_{\alpha i} = n_{\alpha}(x_i)/n_{\alpha}$ . This nonlinear set of equations is solved by Newton's method. The iterative process is continued until the Euclidean norm of the updates after iteration  $k + 1$  becomes less than  $10^{-10}$ .

$$\left[ \sum_{\alpha}^2 \sum_{i=1}^N (g_{\alpha i}^{(k+1)} - g_{\alpha i}^{(k)})^2 / 2N \right]^{\frac{1}{2}} \leq 10^{-10}, \quad (4.1)$$

where  $N$  is the number of nodes in the domain  $d/2 < x < R$ , and  $R$  is the cutoff value for the integrals in Eqs.(3-23). Both the number of nodes  $N$  and the value of  $R$  depend on concentration. We used a uniform mesh in the domain  $d/2 < x < R$ .

Either the charge density,  $\sigma$ , or the electrostatic potential at the electrode,  $\psi_e$ , can be specified and the equations solved. At very low charge densities,  $\sigma$ , or potentials,  $\psi_e$ , we found it convenient to use the MGC density profiles as an initial guess. Once a solution for certain values of the parameters is found, initial estimates at other values for the parameters can be found easily by a first-order continuation technique. Typically, three to five Newton iterations are needed to reach convergence. After convergence was attained, the value of  $\sigma$  or the value of  $\psi_e$ , depending on which quantity was used as the parameter, were computed using Eq.(2.8) or Eq.(2.10) respectively. The agreement with the value of  $\sigma$  or  $\psi_e$  originally used to solve the equations gives an indication of the accuracy of the numerical method. Except for the very low concentration regime, Eq.(2.8)

or (2.10) was satisfied to at least five significant figures. In the most dramatic case treated; 1:1 electrolyte at 0.01 M, the dimensionless Debye distance,  $\kappa_D^{-1}$ , becomes very small and Eq.(2.8) or (2.10) was satisfied to four significant figures only.

In our calculations we have used dimensionless parameters. We express all lengths in units of the diameter  $d$ . The dimensionless surface charge is  $\sigma^* = \sigma d^2/e$ , where  $e$  is the magnitude of the electronic charge. Similarly the dimensionless potential profile is  $\psi^*(x) = \beta e \psi(x)$ . In order to compare with the MC data of Valleau and co-workers, [6] we fixed the value of the plasma parameter to  $\Gamma = \beta e^2/\epsilon d = 1.6809$ . This value corresponds to

$$\epsilon = 78.5, \quad T = 298K \quad \text{and} \quad d = 4.25\text{\AA}.$$

### 1:1 electrolytes

We solved Eq(3.23) for electrolytes ranging from 0.01-2 M and surface charge ranging from 0.05-0.9. In Table I we list the dimensionless diffuse layer potential,  $\beta e \psi(0)$ , where  $\psi(0)$  is the potential drop between the point of closest approach to the surface and infinity. Note that the position of the wall has been shifted to  $x = -d/2$ . In Table I we also display the MC results [6], those of MGC, BGY [11], MPB5 [7] theories and the OZ/LMBW results obtained recently by Plischke and Henderson [15] using the HNC closure. The general agreement of our results with the MC data is quite good. A clearer comparison of our results for 1:1 electrolytes with MC data is given by Fig. 1 where we plot the diffuse layer potential  $\psi^*(0)$  as a function of the reduced charge density  $\sigma^*$ . As reported before by other authors, [11,15] in the low concentration regime, density profiles become very long ranged and special numerical difficulties appear. We believe that the discrepancies between our results and the MC data at  $c = 0.01$  M can be attributed, at least in part, to this cause. The crosses shown in Fig. 1 are the results of Plischke and Henderson [15].

The classical MGC theory, which neglects the finite size of the ions, predicts an interfacial thickness which is greater than that obtained by MC simulations for low surface charge densities, and smaller than that of the MC data for large  $\sigma^*$ . This phenomenon is evident at 1 M concentration. In Fig. 2 we plot the diffuse layer potential as a function of surface charge density for  $c = 1$  M. In that figure we also display the MC data, and the results obtained from the approximations listed in Table I. The agreement of our results with MC is very good and in some cases of comparable accuracy with those obtained by Plischke and Henderson [15] with the OZ/LMBW and the HNC closure. The data available for the MPB5 theory show an excellent agreement with MC data. Unfortunately the data are for low values of  $\sigma^*$  only, and because of the secondary role played by the excluded volume effects in the MPB5 theory, it is not expected that the theory can be applied at higher surface charges where the size effects are very important. The BGY theory of Caccamo et al., Ref.(11), which is very good for low  $\sigma^*$  fails to predict the change in curvature showed by the MC results at intermediate charge densities.

The classical theory of Gouy-Chapman always predict monotonic variation for the density profiles of both coions and counterions. In contrast, for 1:1 electrolytes, the MC



results of Valleau and collaborators [6] for the structure of the RPM double layer exhibit interesting layering effects for high surface charges. In Fig. 3 we present a comparison of our results for the density profiles of a double layer for a bulk density of  $c = 0.1M$  and  $\sigma^* = 0.30$ , with those corresponding to MC simulation and the MGC theory. Our results agree quite well with the MC results. All the profiles showed are monotonic in this case. In Fig. 4 we plot the mean electrostatic profile which correspond to the same condition presented in Fig. 3. Again we obtain very good agreement with the MC results. The MGC theory is relatively succesful in describing both density profiles and mean electrostatic potential at  $c = 0.1M$  and  $\sigma^* = 0.30$ .

In Fig. 5 we present, with solid lines, the counterion and coion density profiles obtained in this work for  $c = 1M$  and  $\sigma^* = 0.42$ . For comparison, in the same figure we show the MC and MGC results. Also shown in the figure are the results obtained by Plischke and Henderson for the OZ/LMBW theory with the MSA closure. It is important to mention at this point that, for this concentration and surface charge, the results of the OZ/LMBW theory with the MSA closure are in very good agreement with those of the same theory when the HNC closure is employed [15]. The MC results clearly show the onset of the formation of a second layer of counterions near  $x/d = 1$ . Since the MGC theory is a point charge theory, it does not predict the layering phenomenon. On the other hand, the OZ/LMBW theory accurately follows the behavior of the MC data. It is interesting to see that the density functional theory presented in this paper is also able to predict the formation of the second layer of counterions. However, the position of the second layer is clearly shifted towards the electrode. The theory also exaggerates the size of the second peak. The coion density profile predicted by the density functional theory agrees quite well with MC data and is almost indistinguishable from that of the OZ/LMBW theory.

At a bulk concentration of  $c = 1M$  and a charge density  $\sigma^* = 0.7$ , a second layer of counterions is clearly formed. In Fig. 6 we compare the density profiles predicted by MGC, OZ/LMBW, and density functional theories with the MC results for that conditions. Again the MGC theory predicts monotonic profiles while the OZ/LMBW theory very well predicts both the position and magnitud of the second layer. Again the density functional theory overemphasize the value of the density of the second layer. As in Fig. 5, the position of this layer is shifted towards the electrode. This can be a consequence of the way in which the GHRM takes into account the hard-core effects. The GHRM predicts, for a hard-sphere fluid near a hard wall, a density profile with a second peak shifted towards the wall when compared with simulation results. See Ref. (30).

The mean electrostatic potential profile wich corresponds to the last conditions presented is shown in Fig. 7. The agreement between the density functional theory and the MC results is very good. The density functional theory is able to predict the presence of a very shallow minimum in this function. A similar minimum is present in the MC results. The mean electrostatic potential function is not very sensitive to the details in the structure of the double layer.

## 2:2 electrolytes

We have computed results of our density functional theory for two concentrations: 0.05 and 0.5 M. In the lower part of Table I we display some results of this work for the diffuse layer potential and compare with those of the theories previously mentioned. We find reasonable agreement with MC data.

In the case of divalent electrolytes, the MC results show the interesting phenomenon of charge inversion. This phenomena, which is a result of both hard-core and electrostatic interactions, consists in the formation of a second layer of coions next to the first layer of counterions. In Fig. 8 we plot density profiles for a double layer at  $c = 0.5M$  and  $\sigma^* = 0.1704$ . Nearly all the counterion charge is concentrated into a thin layer next to the wall. The response of the system to this dipole layer is the formation of a layer of coions within  $x = d$  and  $x = 2d$  approximately. As can be seen in Fig. 8, the density functional theory is predicting the charge inversion phenomenon. We obtained a counterion density profile in very reasonable agreement with MC data. On the other hand, our theory tends to underestimate the magnitude of the maximum in the coion profile. As expected, the MGC theory totally ignores the charge inversion.

In Fig. 9 we show the mean electrostatic potential profile for the same conditions presented in the previous figure. The MC simulations result in a potential profile which is oscillatory with a minimum of about -0.2 just beyond one diameter from the wall. Our density functional theory predicts the oscillatory behavior and is in very good agreement with the MC data.

## V. SUMMARY

We presented a nonlocal free energy density functional theory for the electrical double layer. Within the frame of the grand canonical formalism, we construct a free energy functional of the density distribution. We then separate the short ranged part of the inhomogeneous direct correlation functions which appear in the formalism into a hard-sphere term and a residual term. The residual term contains the correlations arising from the Coulombic interactions between particles in the fluid. The hard-sphere part of the free energy functional is then approximated by a generic functional proposed by Percus [36] as a three dimensional generalization of an inhomogeneous hard-rod system. We used its extension to mixtures due to Vanderlick *et al.* [29]. This generic nonlocal functional requires the specification of two coarse-grain densities. In this work we choose to use the weighting functions proposed by Robledo and Varea [37] and by Fischer and Heinbuch [38] to generate a GHRM functional for the free energy of an inhomogeneous hard-sphere system. In our calculations we approximate the free energy of a bulk hard-sphere mixture with the Carnahan-Starling [47] expression. The residual inhomogeneous direct correlation functions are approximated with those corresponding to the neutral bulk electrolyte which is in equilibrium with the interface. Use is made of the analytical solutions of the MSA

[47].

The GHRM free energy density functional theory described in Sec.III correctly describes the physical features presented by the MC simulations for 1:1 and 2:2 RPM electrolytes. For 1:1 electrolytes the theory predicts the layering of counterions which occurs when the charge of the electrode is increased. Although the theory exaggerates the magnitude of the counterion layering, predicts a diffuse layer potential which is in very good agreement with the MC data. For 2:2 electrolytes, the theory predicts the charge inversion phenomenon and values of the diffuse layer potential which are in good agreement with MC results. In general, there are small quantitative rather than qualitative differences between the MC results for the density profiles and mean electrostatic potential and those obtained in this work.

Even when calculations with the GHRM density functional theory are relatively simple, the theory competes in accuracy with the more sophisticated OZ/LMBW theory [15]. Because of its simplicity, the GHRM theory requires only a small fraction of the computing time used to solve the OZ/LMBW theory. For the 1:1 electrolyte at  $c = 1M$ , our code requires only 240 s of a Cray2 CPU time to calculate solutions and mean electrostatic potential profiles at 15 different values of reduced charge density,  $\sigma^*$ , with a uniform mesh of 241 nodes, for example.

From a density functional formulation similar to that presented here, Fortsmann and collaborators [13] used in the interface ion-ion correlation functions of homogeneous electrolytes with non-neutral compositions. Instead, in our work we are employing a nonlocal GHRM functional for the hard sphere part of the free energy and neutral bulk electrolyte correlation functions for the residual electrostatic part. Use of non-neutral composition residual electrostatic correlations is left for future work.

The results of the GHRM for a hard-sphere system near a hard-wall, reported in Ref.(30) show a poor quantitative agreement with MC results. Since a very good agreement between the functional theory and the MC results for the planar double layer is reported in Sec. IV, one can naturally ask if a fortuitous cancellation of error is occurring when we combine the hard-sphere free energy functional with the MSA solutions for the electrostatic part of direct correlation functions. The answer to this question probably can be given by solving the theory for a more accurate functional for the hard-sphere contribution to the free energy. The SDA of Tarazona [24] seems to be a good option for this purpose. We hope to contribute to the solution of this question in the near future.

## ACKNOWLEDGMENTS

We thank M. Plischke and D. Henderson for sharing their OZ/LMBW with MSA closure prior to publication. L. M.-y-T. and S.H.S. gratefully acknowledge the hospitality extended to them by the Supercomputer Institute. L.M.-y-T. gratefully acknowledges

the partial support given to him by CONACYT, Mexico. The Office of Naval Research, the National Science Foundation, and the Minnesota Supercomputer Institute provided support for this work.

## REFERENCES

1. G. Gouy, *J. Phys.* 9, 451 (1910).
2. D. L. Chapman, *Philos. Mag.* 25, 475 (1913).
3. S. L. Carnie and G. M. Torrie, *Advan. Chem. Phys.* 56, 141 (1984).
4. W. Schmickler and D. Henderson, *Progr. Surf. Sci.* 22, 323 (1986).
5. O. Stern, *Z. Electrochem.* 30, 508 (1924).
6. G. M. Torrie and J. P. Valleau, *J. Chem. Phys.* 73, 5807 (1980); G. M. Torrie, J. P. Valleau, and G. N. Patey, *ibid.* 76, 4615 (1982); J. P. Valleau and G. M. Torrie, *ibid.* 76, 4623 (1982); G. M. Torrie and J. P. Valleau, *J. Phys. Chem.* 86, 3251 (1982).
7. C. W. Outhwaite, *J. Chem. Soc. Faraday Trans. 2* 74, 1214 (1978); S. Levine and C. W. Outhwaite, *ibid.* 74, 1670 (1978); L. B. Bhuiyan, C. W. Outhwaite, and S. Levine, *Chem. Phys. Lett.* 66, 321 (1979); C. W. Outhwaite, L. B. Bhuiyan, and S. Levine *ibid.* 67, 150 (1979); C. W. Outhwaite, L. B. Bhuiyan, and S. Levine, *J. Chem. Soc. Faraday Trans. 2* 76, 1388 (1980); S. Levine, C. W. Outhwaite, and L. B. Bhuiyan, *J. Electroanal. Chem.* 123, 105 (1981); C. W. Outhwaite, L. B. Bhuiyan, and S. Levine, *Chem. Phys. Lett.* 78, 413 (1981); L. B. Bhuiyan, C. W. Outhwaite, and S. Levine, *Mol. Phys.* 42, 1271 (1981); C. W. Outhwaite and L. B. Bhuiyan, *J. Chem. Soc. Faraday Trans. 2* 78, 775 (1982); C. W. Outhwaite and L. B. Bhuiyan, *J. Chem. Soc. Faraday Trans. 2* 79, 707 (1983); C. W. Outhwaite, *ibid.* 79, 1315 (1983); C. W. Outhwaite and L. B. Bhuiyan, *J. Chem. Phys.* 85, 4206 (1986).
8. D. Henderson, F. F. Abraham, and J. A. Barker, *Mol. Phys.* 31, 1291 (1976).
9. L. Blum, *J. Phys. Chem.* 81, 136 (1977); D. Henderson and W. R. Smith, *J. Stat. Phys.* 19, 191 (1978); D. Henderson and L. Blum, *J. Chem. Phys.* 69, 5441 (1978); D. Henderson, L. Blum, and W. R. Smith, *Chem. Phys. Lett.* 63, 381 (1979); D. Henderson and L. Blum, *J. Electroanal. Chem.* 111, 217 (1980); S. L. Carnie, D. Y. C. Chan, D. J. Mitchell, and B. W. Ninham, *J. Chem. Phys.* 74, 1472 (1981); M. Lozada-Cassou, R. Saavedra-Barrera, and D. Henderson, *ibid.* 77, 5150 (1982); M. Lozada-Cassou and D. Henderson, *J. Phys. Chem.* 87, 2821 (1983); J. Barojas, D. Henderson, and M. Lozada-Cassou, *ibid.* 87, 4547 (1983); *ibid.* 88, 2926 (1984); S. L. Carnie, *Mol. Phys.* 54, 509 (1985); L. Mier y Teran, E. Diaz-Herrera, M. Lozada-Cassou, and D. Henderson, *J. Phys. Chem.* 92, 6408 (1988).
10. T. L. Croxton, D. A. McQuarrie, *Chem. Phys. Lett.* 68, 489 (1979); *Mol. Phys.* 42, 141 (1981); D. Henderson, L. Blum, L. B. Bhuiyan, *Mol. Phys.* 43, 1185 (1981); L. Blum, J. Hernando, and J. L. Lebowitz, *J. Phys. Chem.* 81, 2825 (1983).
11. C. Caccamo, G. Pizzimenti, and L. Blum, *Phys. Chem. Liquids* 14, 311 (1985); *J. Chem. Phys.* 84, 3327 (1986); E. Bruno, C. Caccamo, and G. Pizzimenti, *ibid.* 86, 5101 (1987).
12. P. Nielaba and F. Forstmann, *Chem. Phys. Lett.* 117, 46 (1985); P. Nielaba, T. Alts,

- B. Daguanno, and F. Forstmann, *Phys. Rev. A* 34, 1505 (1986); B. Daguanno, P. Nielaba, T. Alts, and F. Forstmann, *J. Chem. Phys.* 85, 3476 (1986).
13. T. Alts, P. Nielaba, B. Daguanno, and F. Forstmann, *Chem. Phys.* 111, 223 (1987).
  14. R. Kjellander and S. Marcelja, *Chem. Phys. Lett.* 112, 49 (1984); *J. Chem. Phys.* 82, 2122 (1985); *Chem. Phys. Lett.* 127, 462 (1986).
  15. M. Plischke and D. Henderson, *J. Chem. Phys.* 88, 2712 (1988); 90, 5738 (1989).
  16. R. Lovett, C. Y. Mou, and F. P. Buff, *J. Chem. Phys.* 65, 570 (1976); M. Wertheim, *ibid.* 65, 2377 (1976).
  17. J. D. van der Waals and Ph. Kohnstamm, *Lehrbuch der Thermodynamik*, (Maas and van Suchtelen, Leipzig, 1908), Vol. 1.
  18. G. Stell, in "The Equilibrium Theory of Classical Fluids", edited by H. L. Frisch and J. L. Lebowitz, (Benjamin, New York, 1964), pp. II71-II226.
  19. J. K. Percus, in "The Equilibrium Theory of Classical Fluids", edited by H. L. Frisch and J. Lebowitz, (Benjamin, New York, 1964), pp. II30-II70.
  20. C. Ebner, W. F. Saam, and D. Stroud, *Phys. Rev. A* 14, 2264 (1976).
  21. V. Bongiorno and H. T. Davis, *Phys. Rev. A* 12, 2213(1975); V. Bongiorno, L. E. Scriven, and H. T. Davis, *J. Colloid Interf. Sci.* 57, 462(1976); H. T. Davis and L. E. Scriven, *Adv. Chem. Phys.* 49, 357 (1982).
  22. R. Evans, *Adv. in Phys.* 28, 143 (1979).
  23. See, e.g., S. Nordholm, J. Gibson, and M. A. Hooper, *J. Stat. Phys.* 28, 391 (1982).
  24. P. Tarazona, *Phys. Rev. A* 31, 2672 (1985); 32, 3148 (1985).
  25. W. A. Curtin and N. W. Ashcroft, *Phys. Rev. A* 32, 2909 (1985); *Phys. Rev. Lett.* 56, 2775 (1986).
  26. T. F. Meister and D. M. Kroll, *Phys. Rev. A* 31, 4055 (1985).
  27. G. S. Heffelfinger, Z. Tan, U. Marini Bettolo Marconi, F. van Swol, and K. E. Gubbins, *Molecular Simulation* 2, 393 (1989).
  28. P. C. Ball and R. Evans, *J. Chem. Phys.* 89,4412 (1988).
  29. T. K. Vanderlick, H.T. Davis and J.K. Percus, *J. Chem. Phys.* (to appear 1989).
  30. T. K. Vanderlick, L. E. Scriven and H. T. Davis, *J. Chem. Phys.* 90, 2422 (1989).
  31. P. Tarazona, U. Marini Bettolo Marconi, and R. Evans, *Mol. Phys.* 60, 573, (1987).
  32. B. K. Peterson, K. E. Gubbins, G. S. Heffelfinger, U. Marini Bettolo Marconi, and F. van Swol, *J. Chem. Phys.* 88, 6487 (1988).
  33. P. Ball and R. Evans, *Mol. Phys.* 63, 159 (1988).
  34. E. J. Boyle, L. E. Scriven, and H. T. Davis, *J. Chem. Phys.* 86, 2309 (1987).
  35. Z. Tan, U. Marini Bettolo Marconi, F. van Swol, and K. E. Gubbins, *J. Chem. Phys.* 90, 3704 (1989).
  36. J. K. Percus, *J. Chem. Phys.* 75, 1316 (1981).
  37. A. Robledo and C. Varea, *J. Stat. Phys.* 26, 513 (1981).
  38. J. Fischer and U. Heinbuch, *J. Chem. Phys.* 88, 1909 (1988).
  39. J. K. Percus, *J. Stat. Phys.* 15, 505 (1976).
  40. T. Morita and K. Hiroike, *Prog. theor. Phys.* 25, 537 (1961).
  41. C. DeDominicis, *J. Math. Phys.* 3, 983 (1962).
  42. F. H. Stillinger and F.P. Buff, *J. Chem. Phys.*, 37, 1(1962).
  43. J. L. Lebowitz and J. K. Percus, *J. Math. Phys.* 4, 116 (1963).

44. W. F. Saam and C. Ebner, Phys. Rev. A 15, 2566 (1977).
45. N. D. Mermin, Phys. Rev. A 137, 1441 (1965).
46. P. Hohenberg and W. Kohn, Phys. Rev. B 136, 864 (1964).
47. N. F. Carnahan and K. E. Starling, J. Chem. Phys. 51, 635 (1969); *ibid* 53, 600 (1970).
48. G. A. Mansoori, N. F. Carnahan, K. E. Starling, and T. W. Leland, J. Chem. Phys. 54, 1523 (1971).
49. J. S. Barker and D. Henderson, Rev. Mod. Phys. 48, 587 (1976).
50. E. Waismann and J. L. Lebowitz, J. Chem. Phys. 56, 3086 (1972); 56, 3093 (1972).
51. G. Strang and G. Fix, An Analysis of the Finite Element Method (Prentice Hall, Englewood Cliffs. New Jersey, 1973).
52. L. Mier y Teran, A. H. Falls, L. E. Scriven, and H. T. Davis, Proceedings 8th Symposium of Thermophysical Properties, ed. J. V. Sengers, American Society of Mechanical Engineers, New York, (1982) Vol. 1, pp. 45-56.
53. L. Mier y Teran, E. Fernandez-Fassnacht, and S. Quinones, Phys. Lett. 107 A, 329 (1985); L. Mier y Teran, E. Fernandez-Fassnacht, Rev. Mex. Fis. 32, S241 (1986); Phys. Lett. 117 A, 43 (1986).
54. L. Mier y Teran, E. Diaz-Herrera, M. Lozada-Cassou., and R. Saavedra-Barrera, J. Comput. Phys. (in press)

## FIGURE CAPTIONS

Fig. 1 Reduced diffuse layer potential,  $\beta e\psi(0)$ , as a function of the charge density,  $\sigma d^2/e$ , for 1:1 electrolytes. Solid lines represent the results of the GHRM functional density theory presented here for 0.01 M, 0.1 M, 1 M and 2 M. Open circles, solid squares, solid circles and open squares are the corresponding MC results. The crosses (x) are the results of the OZ/LMBW theory with the HNC closure, Ref.(15).

Fig. 2 Reduced diffuse layer potential,  $\beta e\psi(0)$ , as a function of charge density,  $\sigma d^2/e$ , for 1 M, 1:1 electrolytes. The solid line represents results of the functional density theory. Solid circles are the MC results of Valleau and collaborators, Ref. (6). Solid squares correspond to the MPB5 theory [7], open circles to the BGY theory [11], and open squares to the OZ/LMBW theory with the HNC closure, Ref. (15).

Fig. 3 Reduced density profiles,  $n(x)/n$ , for a 1:1 electrolyte at  $c = 0.1M$  and  $\sigma^* = 0.30$ . The dots are the MC results. The dashed lines correspond to the MGC theory and the solid lines to this work. Note that the wall is at  $x = -d/2$ .

Fig. 4. Reduced mean electrostatic potential profile for a 1:1 electrolyte at  $c = 0.1M$  and  $\sigma^* = 0.3$ . All symbols as in Fig. 3.

Fig. 5 Reduced density profiles,  $n(x)/n$ , for a 1:1 electrolyte at  $c = 1M$ ,  $\sigma^* = 0.42$ . The

dots are the MC results. The dashed lines correspond to the MGC theory, the dot dashed lines to the OZ/LMBW theory with the MSA closure, and the solid lines to this work.

Fig. 6 Reduced density profiles,  $n(x)/n$ , for a 1:1 electrolyte at  $c = 1M$  and  $\sigma^* = 0.7$ . All symbols as in Fig. 5.

Fig. 7 Reduced mean electrostatic potential profile for a 1:1 electrolyte at  $c = 1M$  and  $\sigma^* = 0.7$ . The dots are the MC results. The dashed lines correspond to the MGC theory and the solid line to this work.

Fig. 8 Reduced density profiles,  $n(x)/n$ , for a 2:2 electrolyte at  $c = 0.5M$  and  $\sigma^* = 0.1704$ . The dots are the MC results. The dashed lines correspond to the MGC theory and the solid lines to this work.

Fig. 9 Reduced mean electrostatic potential profile for a 2:2 electrolyte at  $c = 0.5M$  and  $\sigma^* = 0.1704$ . The dots are the MC results. The dashed line corresponds to the MGC theory and the solid line to this work.

TABLE I. Diffuse layer potential

| C                  | $\sigma^*$ | MGC  | MC <sup>a</sup> | BGY <sup>b</sup> | MPB5 <sup>c</sup> | PH <sup>d</sup> | This work |
|--------------------|------------|------|-----------------|------------------|-------------------|-----------------|-----------|
| 1 : 1 electrolytes |            |      |                 |                  |                   |                 |           |
| 0.01M              | 0.10       | 5.44 | 5.05(0.05)      | —                | 5.08              | 4.56            | 5.26      |
| 0.1M               | 0.30       | 5.34 | 4.63(0.03)      | 5.0              | 4.74              | 4.37            | 4.76      |
| 1M                 | 0.10       | 1.4  | 1.09(0.06)      | 1.055            | 1.03              | 1.06            | 1.03      |
|                    | 0.25       | 2.79 | 2.13(0.05)      | 2.31             | 2.10              | 2.22            | 2.18      |
|                    | 0.42       | 3.74 | 3.08(0.1)       | 3.46             | 3.02              | 3.23            | 3.23      |
|                    | 0.55       | 4.26 | 4.15(0.15)      | 4.21             | —                 | 4.22            | 4.12      |
|                    | 0.60       | 4.43 | 4.38(0.11)      | 4.48             | —                 | 4.68            | 4.52      |
|                    | 0.70       | 4.74 | 5.71(0.14)      | 5.02             | —                 | 5.76            | 5.41      |
| 2M                 | 0.396      | 2.99 | 2.29(0.09)      | 2.303            | —                 | 2.29            | 2.19      |
| 2 : 2 electrolytes |            |      |                 |                  |                   |                 |           |
| 0.05M              | 0.20       | 2.61 | 1.33(0.02)      | 1.81             | 1.36              | 1.18            | 1.59      |
| 0.5M               | 0.1704     | 1.36 | 0.63(0.04)      | 0.64             | 0.537             | 0.69            | 0.57      |

<sup>a</sup> G. M. Torrie and J. P. Valleau, Ref. (6); 1980 and 1982. Statistical uncertainty is shown in parenthesis.

<sup>b</sup> C. Caccamo, G. Pizzimenti, and L. Blum, Ref. (11); 1986.

<sup>c</sup> C. W. Outhwaite and L.B. Bhuiyan, Ref. (7); 1986.

<sup>d</sup> M. Plischke and D. Henderson, Ref. (15); 1988.



Fig 1

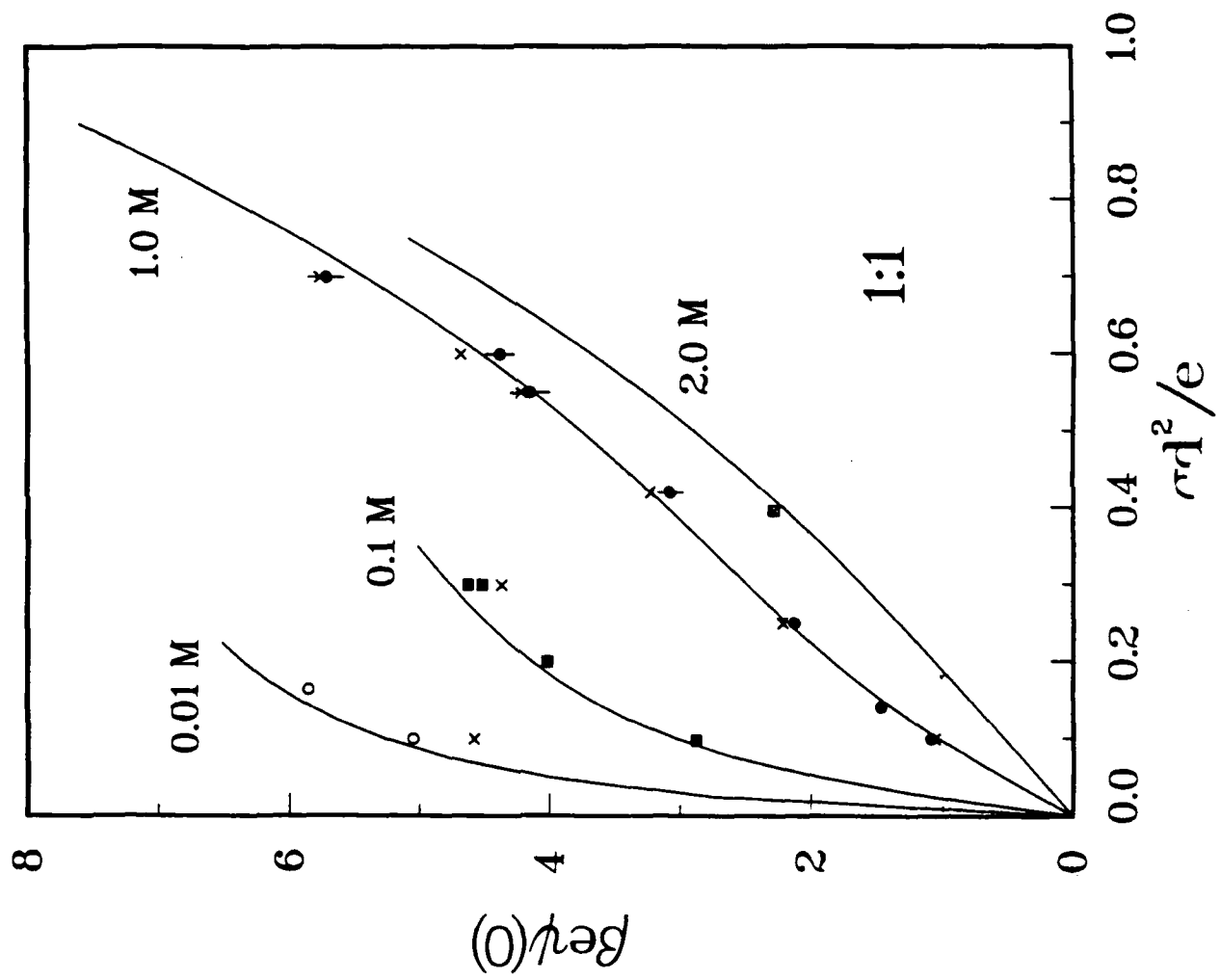


Fig 2

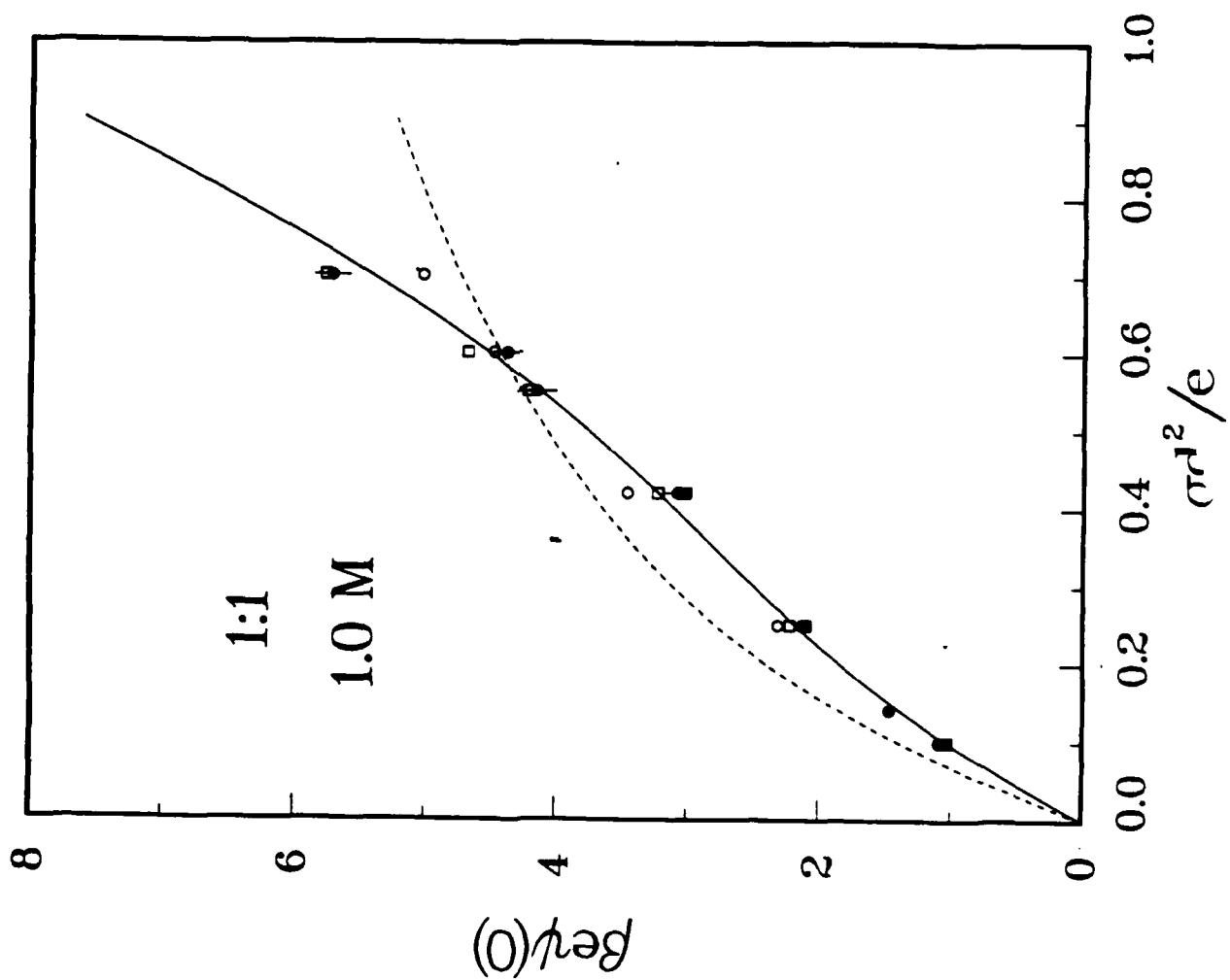


Fig. 1

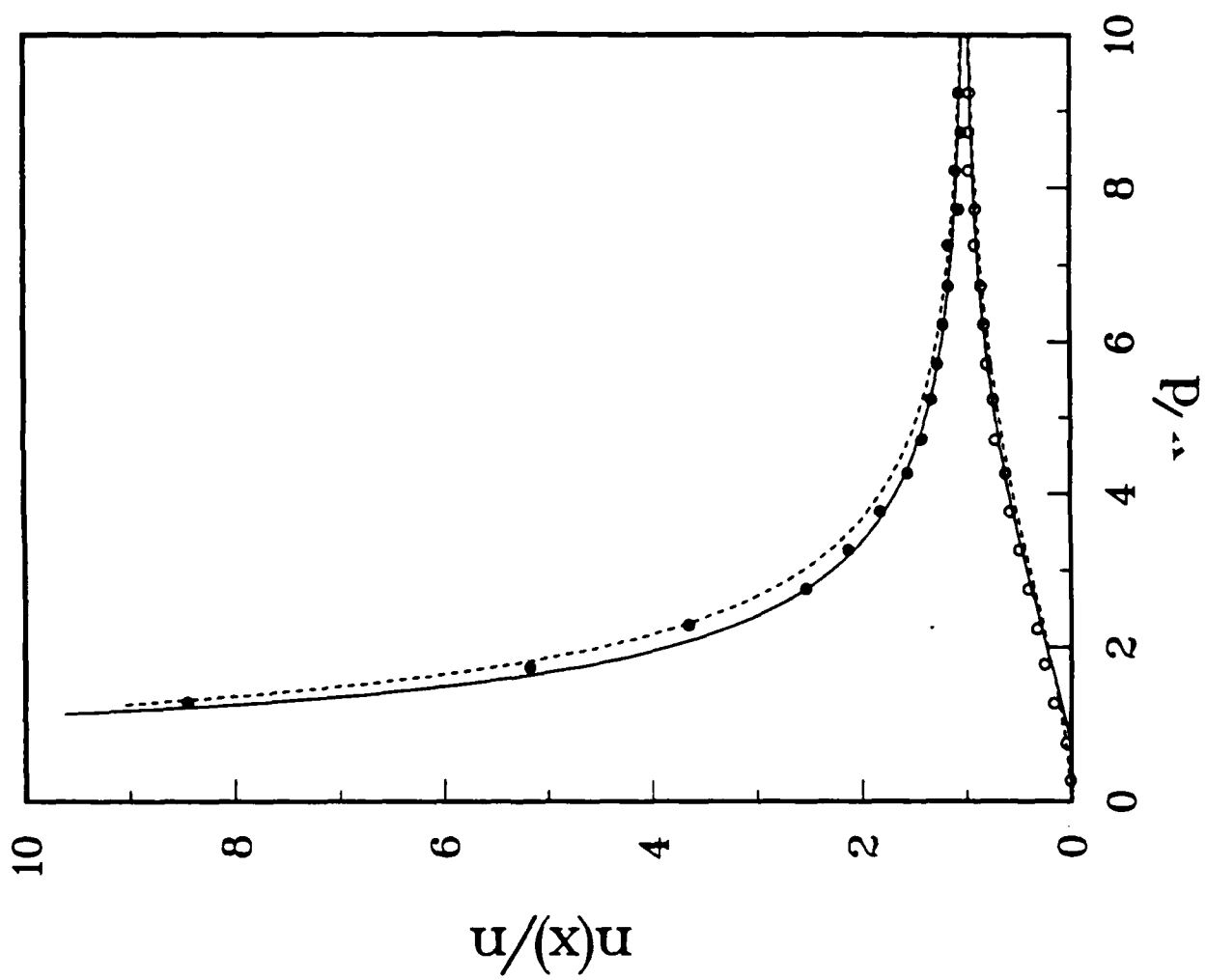


Fig. 4

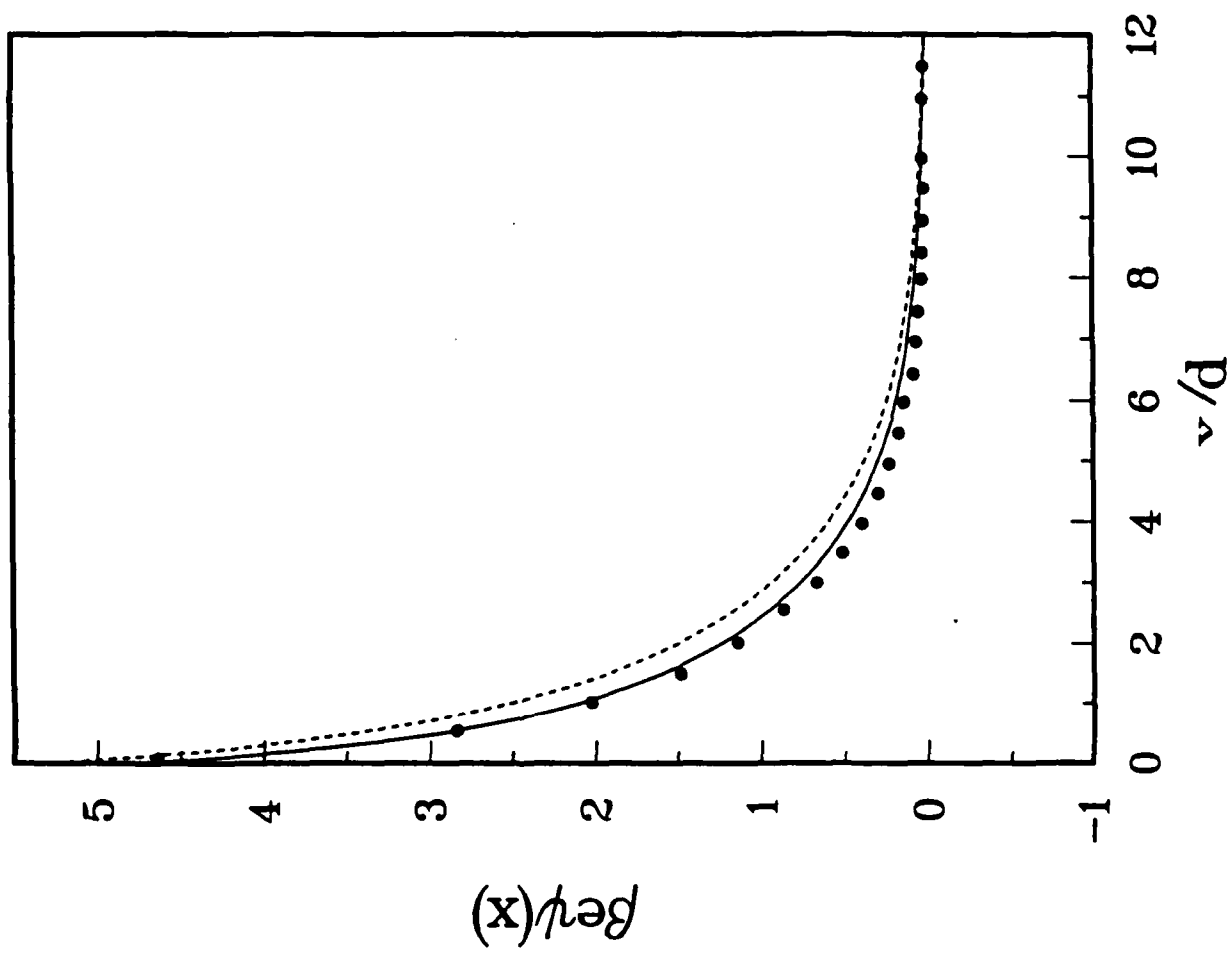


Fig 5

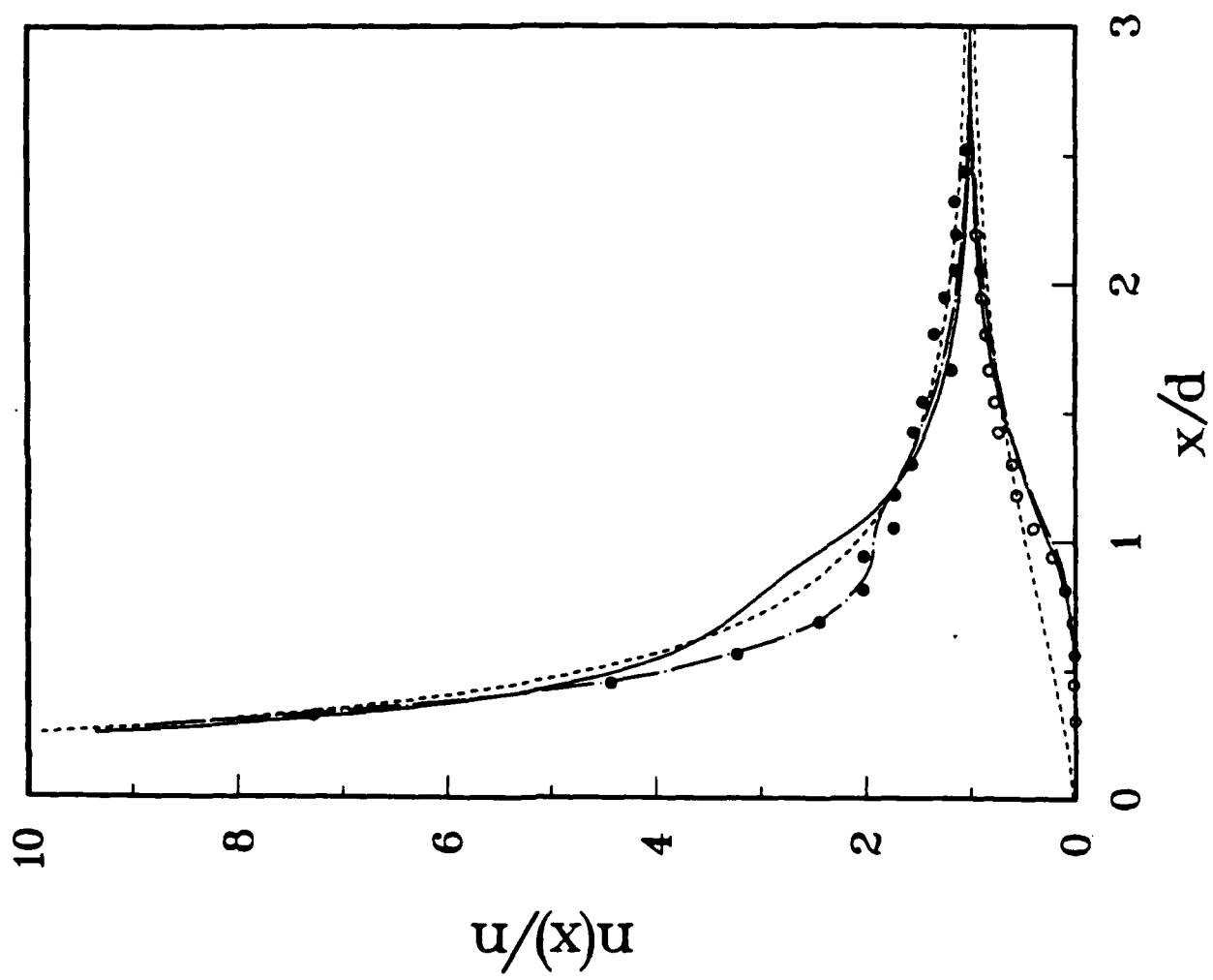


Fig. 6

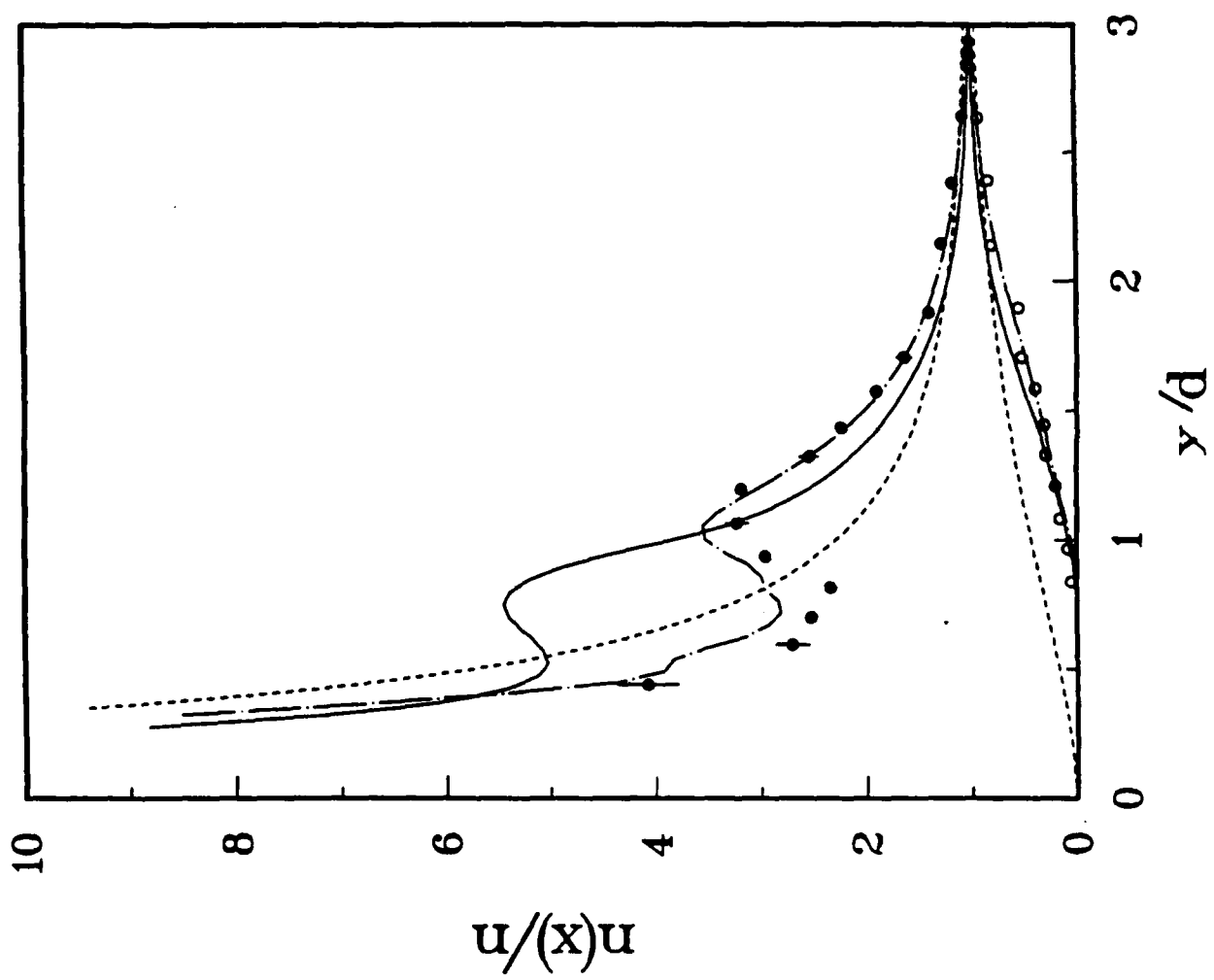


Fig. 7

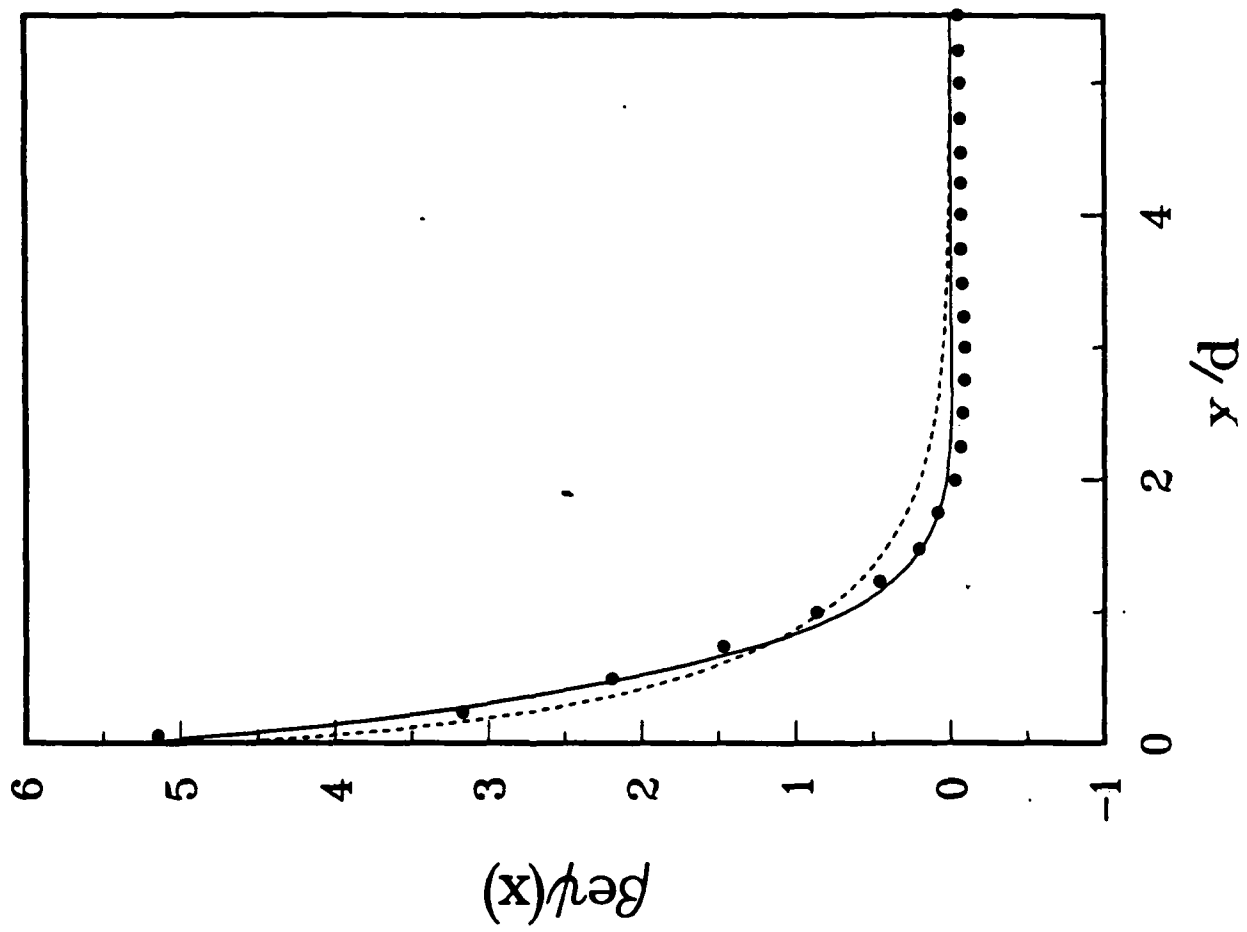


Fig. 8

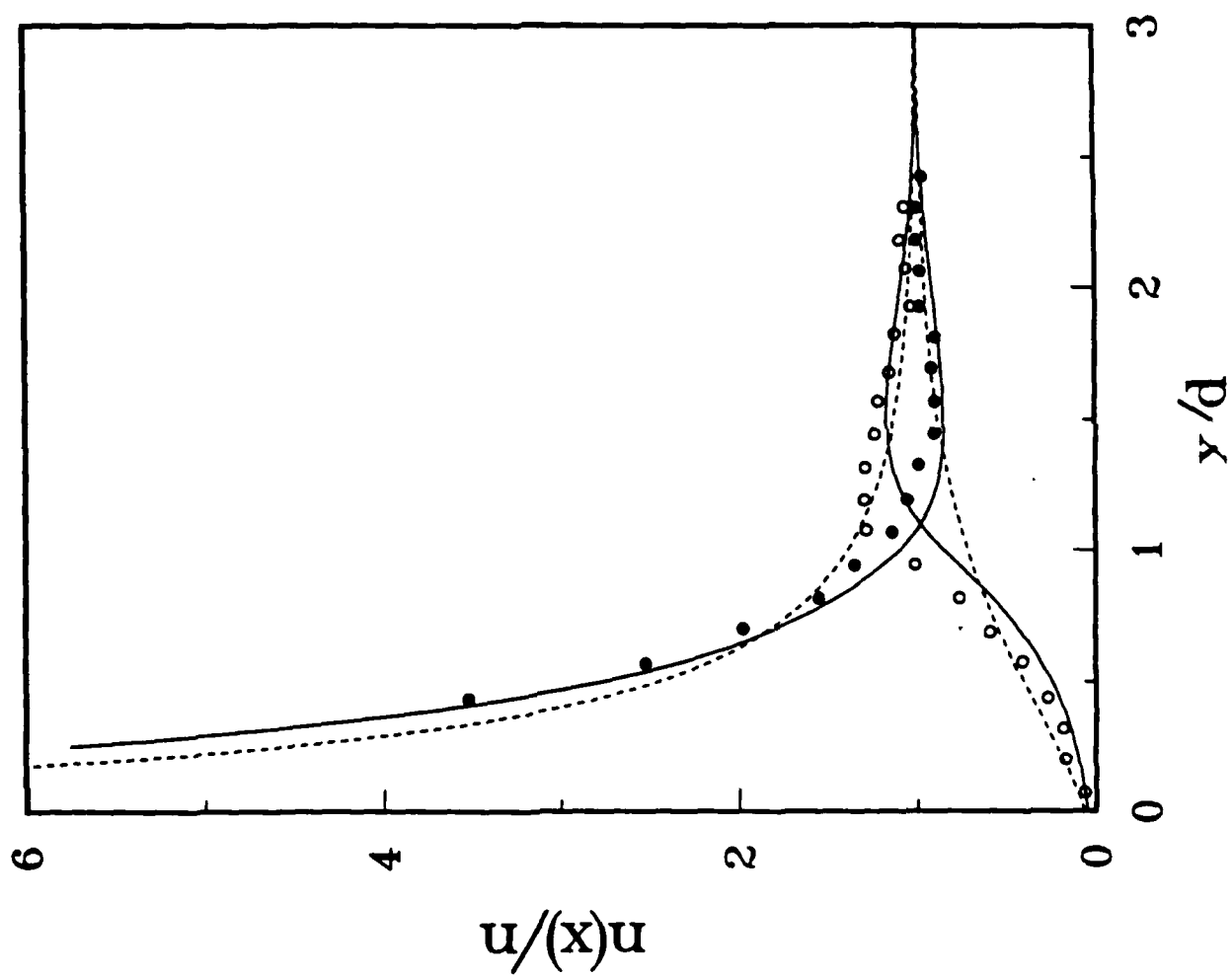




Fig. 9

